

RECEIVED

NC 14

GOVT. DOC.

BUSINESS, SCIENCE  
& TECHNOLOGY DEPT.

Wright Field Technical Report

TECHNICAL NOTES

NATIONAL ADVISORY COMMITTEE FOR AERONAUTICS

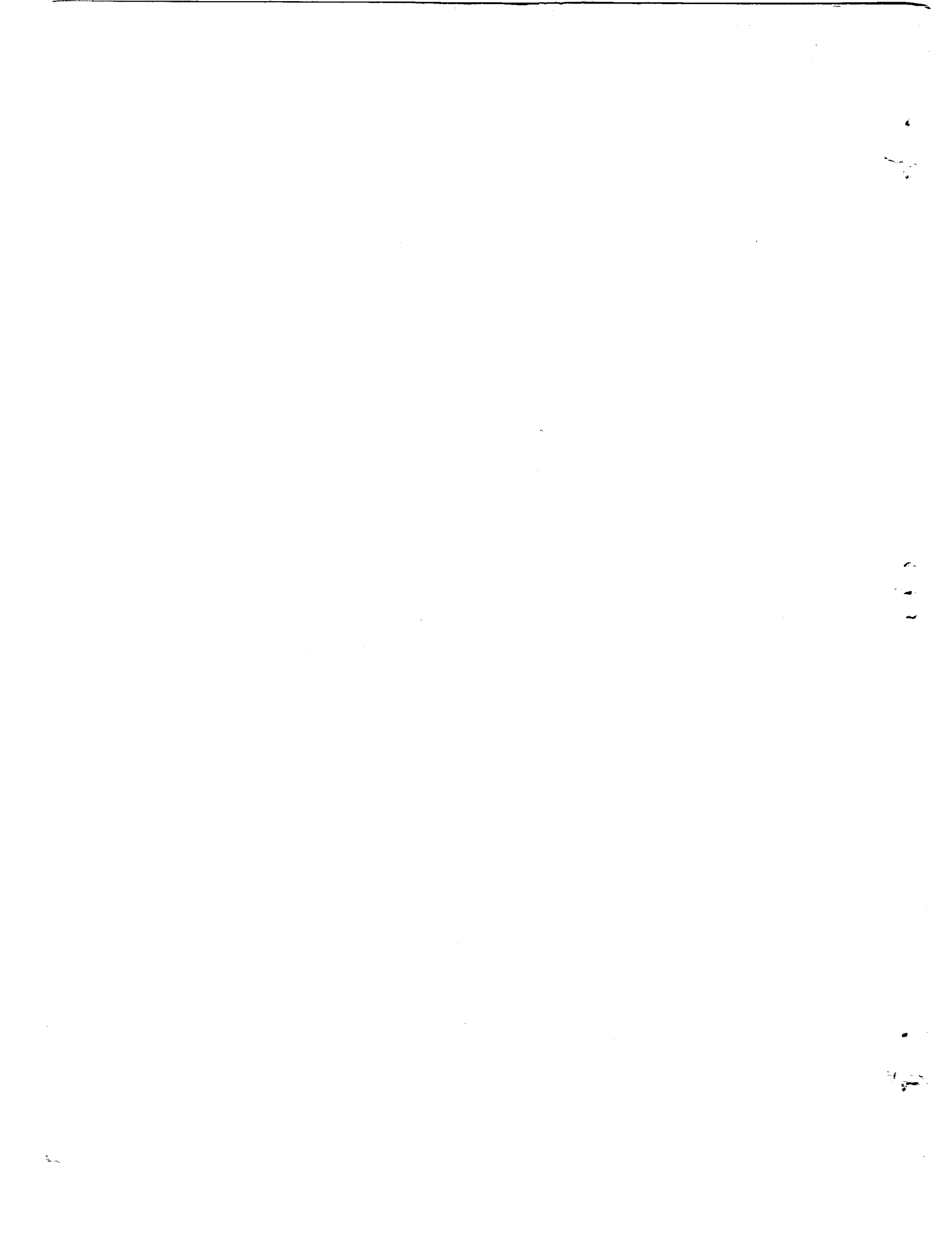
No. 614

FUSELAGE-DRAG TESTS IN THE VARIABLE-DENSITY WIND TUNNEL:  
STREAMLINE BODIES OF REVOLUTION, FINENESS RATIO OF 5

By Ira H. Abbott  
Langley Memorial Aeronautical Laboratory

Washington  
September 1937

BUSINESS, SCIENCE  
& TECHNOLOGY DEPT.,



NATIONAL ADVISORY COMMITTEE FOR AERONAUTICS

TECHNICAL NOTE NO. 614

FUSELAGE-DRAG TESTS IN THE VARIABLE-DENSITY WIND TUNNEL:  
STREAMLINE BODIES OF REVOLUTION, FINENESS RATIO OF 5

By Ira H. Abbott

SUMMARY

Results are presented of drag tests of six bodies of revolution with systematically varying shapes and with a fineness ratio of 5. The forms were derived from source-sink distributions, and formulas are presented for the calculation of the pressure distributions of the forms. The tests were made in the N.A.C.A. variable-density tunnel over a range of values of Reynolds Number from about 1,500,000 to 25,000,000. The results show that the bodies with the sharper noses and tails have the lowest drag coefficients, even when the drag coefficients are based on the two-thirds power of the volume. The data show the most important single characteristic of the body form to be the tail angle, which must be fine to obtain low drag.

INTRODUCTION

The National Advisory Committee for Aeronautics is conducting an investigation of fuselage drag at large values of the Reynolds Number. The first phase of the investigation is the study of streamline bodies of revolution to obtain data on basic forms that can be modified to obtain fuselages of practical shape for particular types of airplanes.

Tests were made of six streamline bodies of revolution with systematically varying shapes and a fineness ratio of 5. The tests were made in the fall of 1935 in the N.A.C.A. variable-density wind tunnel. The results cover a range of Reynolds Numbers from about 1,500,000 to 25,000,000.

## DERIVATION OF STREAMLINE FORMS

The streamline forms were derived from systematically varied source-sink distributions (references 1 and 2) covering a range of shapes in which it was thought that the lowest drag forms for the selected fineness ratio of 5 would be found. The type of source-sink distribution used is shown in figure 1. The abscissas of the sources are denoted by  $\xi$ , the intensity of the sources per unit length by  $f(\xi)$  in which positive values of  $f(\xi)$  denote sources and negative values, sinks. The condition that makes the stream from the sources self-contained is expressed by the equation

$$\int_0^l f(\xi) d\xi = 0 \quad (1)$$

The stream function is taken as the quantity of fluid flowing inside a circle perpendicular to the axis and having its center on the axis (fig. 1). In the computation of the stream function  $\psi_1$  due to the sources, the amount of fluid delivered by the sources upstream from the circle is deducted from the quantity passing through the circle. The stream function of the sources is then given by the formula

$$\psi_1 = -\frac{1}{2} \int_0^l f(\xi) \left(1 + \frac{x - \xi}{r}\right) d\xi \quad (2)$$

where  $r = \sqrt{(x - \xi)^2 + y^2}$  (reference 2).

To this stream function must be added that due to the superimposed parallel flow

$$\psi_2 = V \pi y^2 \quad (3)$$

The condition defining the surface of the body about which the flow takes place is

$$\psi_1 + \psi_2 = \psi = 0 \quad (4)$$

The source distributions used are shown in figure

$\Sigma(a,b)$  and the defining constants are given in table I. The integration of equation (2) for the type of source distribution used and the condition

$$\int_0^f f(\xi) d\xi = 1 \quad \int_{\xi}^1 f(\xi) d\xi = -1$$

results in the following equation:

$$\begin{aligned} \psi_1 &= \frac{1}{2ef} \left[ r_e(e+x) - e^2 - xr_o - y^2 \ln \frac{r_e + e - x}{r_o - x} \right] \\ &+ \frac{1}{2(f-e)} \left[ 2(r_f - r_e) - \frac{(f-e)^2}{f} + \frac{1}{f} \left\{ r_e(e+x) - r_f(f+x) + y^2 \ln \frac{r_f + f - x}{r_e + e - x} \right\} \right] \\ &+ \frac{1}{2(h-g)(1-g)} \left[ (h-g)^2 + 2g(r_h - r_g) - r_h(h+x) + r_g(g+x) + y^2 \ln \frac{r_h + h - x}{r_g + g - x} \right] \\ &+ \frac{1}{2(1-g)(1-h)} \left[ (1-h)^2 - 2(r_1 - r_h) + r_1(1+x) - r_h(h+x) - y^2 \ln \frac{r_1 + 1 - x}{r_h + h - x} \right] \end{aligned} \quad (5)$$

where

$$r_o = \sqrt{x^2 + y^2}$$

$$r_e = \sqrt{(x - e)^2 + y^2}$$

$$r_f = \sqrt{(x - f)^2 + y^2}$$

$$r_g = \sqrt{(x - g)^2 + y^2}$$

$$r_h = \sqrt{(x - h)^2 + y^2}$$

$$r_1 = \sqrt{(x - 1)^2 + y^2}$$

The formulas for the speeds of flow due to the source distribution normal to the axis ( $v$ ) and parallel to the axis ( $u$ ) are as follows:

$$\begin{aligned}
 v = & \frac{1}{4\pi y} \left\{ \frac{2}{ef} \left( \frac{xe - x^2 - y^2}{r_e} + \frac{x^2 + y^2}{r_o} \right) + \frac{2}{f - e} \left( \frac{f - x}{r_f} - \frac{e - x}{r_e} \right) \right. \\
 & - \frac{2}{f(f - e)} \left( \frac{xf - x^2 - y^2}{r_f} - \frac{xe - x^2 - y^2}{r_e} \right) + \frac{2g}{(h - g)(1 - g)} \\
 & \left( \frac{h - x}{r_h} - \frac{g - x}{r_g} \right) - \frac{2}{(h - g)(1 - g)} \left( \frac{xh - x^2 - y^2}{r_h} - \frac{xg - x^2 - y^2}{r_g} \right) \\
 & \left. + \frac{2}{(1 - g)(1 - h)} \left( \frac{2x - x^2 - y^2 - 1}{r_1} - \frac{xh - x^2 - y^2 - h + x}{r_h} \right) \right\} \quad (6)
 \end{aligned}$$

$$\begin{aligned}
 u = & \frac{xy}{y} - \frac{1}{4\pi} \left\{ \frac{2}{ef} \left( \frac{x^2(e - x)}{y^2 r_o} + \frac{xe^3}{y^2 r_o} - \frac{e+x}{r_o} + \frac{x}{r_o} + \ln \frac{e - x + r_e}{r_o - x} \right) \right. \\
 & + \frac{2}{f - e} \left( \frac{xf - x^2 - y^2}{y^2 r_f} - \frac{xe - x^2 - y^2}{y^2 r_e} \right) \\
 & - \frac{2}{f(f - e)} \left( \frac{x^2(f - x)}{y^2 r_f} - \frac{x^2(e - x)}{y^2 r_e} - \frac{f + x}{r_f} + \frac{e + x}{r_e} + \ln \frac{f - x + r_f}{e - x + r_e} \right) \\
 & + \frac{2g}{(h - g)(1 - g)} \left( \frac{xh - x^2 - y^2}{y^2 r_h} - \frac{xg - x^2 - y^2}{y^2 r_g} \right) \\
 & - \frac{2}{(h - g)(1 - g)} \left( \frac{x^2(h - x)}{y^2 r_h} - \frac{x^2(g - x)}{y^2 r_g} - \frac{h + x}{r_h} + \frac{g + x}{r_g} + \ln \frac{h - x + r_h}{g - x + r_g} \right) \\
 & + \frac{2}{(1 - g)(1 - h)} \left( \frac{x(2x - x^2 - 1) + y^2}{y^2 r_1} - \frac{x(xh - x^2 - h + x) + y^2}{y^2 r_h} - \frac{l + x}{r_1} + \frac{h + x}{r_h} \right. \\
 & \left. + \ln \frac{l - x + r_1}{h - x + r_h} \right\} \quad (7)
 \end{aligned}$$

It is evident that a group of body surfaces of different fineness ratios can be obtained from one source distribution by choosing different values for the superimposed parallel flow. The maximum diameter of the bodies to be derived was arbitrarily chosen as one-fifth of the length of the source distribution. The speed  $V$  of the superimposed parallel flow to satisfy this condition was determined as follows:

The station  $x$  of the maximum diameter of the body was found by determining from equation (6) the value of  $x$  at which the velocity  $v$  is zero at a value of  $y$  corresponding to the selected maximum radius of the body. The stream function  $\Psi_1$  was then computed for these coordinates by means of equation (5). The required value of  $V$  was then readily determined from equations (3) and (4).

The coordinates of the surfaces of the bodies given in table II were obtained by computing a number of values of  $\Psi_1$  and  $\Psi_2$  corresponding to selected values of  $x$  and  $y$ , and graphically solving equation (4).

This graphical solution (reference 2) consists of plotting curves of  $\Psi_1$  for the condition  $x = \text{constant}$  against  $y$ . The intersections of these curves with that of equation (3) determine the coordinates  $x$  and  $y$  of points on the surface of the body.

In general, the nose and tail points of the body will not fall at  $x = 0$  and  $x = 1$ . For the range of source distributions used, however, the tail points were not appreciably displaced from the point  $x = 1$  and are considered to occur at that point. The nose points, however, are appreciably upstream from the point  $x = 0$  and are not readily determined with sufficient accuracy by the foregoing methods. These points were determined by finding the point on the  $x$  axis where the velocity from the source distribution is equal and opposite to that of the superimposed flow. This point was determined from a simplified form of equation (7) derived to hold on the  $x$  axis in the neighborhood of  $x = 0$ . The fineness ratios of the forms obtained are slightly greater than 5 because of this extension of the nose ahead of the point  $x = 0$ .

The ordinates of the ten forms computed are given in table II and the outlines of the forms are shown in figure 3. Each form is designated by a number of three digits which indicate in a general way the nose shape, the tail fullness, and the tail angle.

The theoretical pressure distribution over the surface of the body or in the field about the body can be obtained from Bernoulli's equation and the velocities  $v$  and  $u$  computed from equations (6) and (7). The total velocity at any point is found by adding vectorially these velocities to the velocity  $V$  of the superimposed parallel flow. The theoretical pressure distribution about form 111 has been computed and is shown in figure 4. It can be seen that the points of discontinuity of the source-distribution curve have no marked direct effect on the fairness of the pressure-distribution curve.

#### MODELS AND TESTS

Aluminum-alloy models were made of forms 111, 221, 222, and 332. The models were 8 inches in maximum diameter and were carefully finished to prevent drag increases due to surface roughness (references 3 and 4). Each model was built in two sections, the division being made at the maximum diameter to allow the various nose and tail portions to be combined to form models of different shape. In this way models approximating the shapes of any of the remaining six computed forms could be obtained if tests of these forms were found to be desirable as a result of the tests of the original four models. Tests were actually obtained in this way of forms 121 and 211. The other four forms were not tested because the results indicated that they would have less favorable drag characteristics than the best tested forms.

The models were tested at zero yaw and pitch in the N.A.C.A. variable-density wind tunnel (reference 5) at six values of the Reynolds Number, based on the model length, from about 1,500,000 to 25,000,000. The test methods and corrections applied to the results are described in references 3 and 4. The precision of the tests was as described in reference 4 except that the uncertainty of the balance calibration mentioned therein had been eliminated by the use of an improved drag balance.

#### RESULTS AND DISCUSSION

Drag coefficients for the six models tested based both on the cross-sectional area  $C_{D_A}$  and the two-thirds

power of the volume  $C_D$  are shown plotted against Reynolds Number in figure 5. The bodies with the sharper noses and tails have the lowest drag coefficients even when the coefficients are based on the two-thirds power of the volume. The data show the most important single characteristic of the body form to be the tail angle, which must be fine to obtain low drag.

Values of the drag coefficient corrected to an effective value of the Reynolds Number of 66,000,000 from the test value of the Reynolds Number of 25,000,000 are tabulated in table III. The correction (reference 6) allows for the decrease in skin-friction drag at the effective value of the Reynolds Number below that for the test value of the Reynolds Number. The correction is made by multiplying the test values of the drag coefficients by a factor, which is taken as 0.875 for a test value of the Reynolds Number of 25,000,000. The corrected values of the drag coefficient are believed to be more nearly applicable to flight at the effective Reynolds Number than the test values at the test Reynolds Number.

The fuselage size for some airplanes, particularly small ones, is largely determined by the cross-sectional area required by the selected seating arrangement. In such cases a fuselage shape such as 111 may save an appreciable part of the fuselage drag as compared with a more conventional shape such as 222. In the case of other airplanes, such as large transports, the longitudinal distribution of fuselage volume becomes of considerable importance, and the fuselage size may be determined by considerations other than that of maximum cross-sectional area. Under these circumstances a careful analysis is required to select the proper form to give lowest drag. Such an analysis is hampered by the lack of knowledge of several factors including the variation of drag with fineness ratio, a study of which constitutes the next part of the N.A.C.A. investigation of fuselage drag.

Langley Memorial Aeronautical Laboratory,  
National Advisory Committee for Aeronautics,  
Langley Field, Va., August 5, 1937.

## REFERENCES

1. Fuhrmann, G.: Theoretische und experimentelle Untersuchungen an Ballonmodellen. Jahrbuch der Motorluftschiff-Studiengesellschaft. Julius Springer (Berlin), 1911-1912, S.65.
2. Prandtl, L.: Applications of Modern Hydrodynamics to Aeronautics. T.R. No. 116, N.A.C.A., 1921.
3. Abbott, Ira H.: Airship Model Tests in the Variable Density Wind Tunnel. T.R. No. 394, N.A.C.A., 1931.
4. Abbott, Ira H.: The Drag of Two Streamline Bodies as Affected by Protuberances and Appendages. T.R. No. 451, N.A.C.A., 1932.
5. Jacobs, Eastman N., and Abbott, Ira H.: The N.A.C.A. Variable-Density Wind Tunnel. T.R. No. 416, N.A.C.A., 1932.
6. Jacobs, Eastman N., and Sherman, Albert: Airfoil Section Characteristics as Affected by Variations of the Reynolds Number. T.R. No. 586, N.A.C.A., 1937.

TABLE I  
CONSTANT DEFINING THE SOURCE-SINK DISTRIBUTIONS USED

Form	e	f	g	h
111	0.050000	0.333333	0.400000	0.700000
121	.050000	.333333	.525000	.775000
122	.050000	.333333	.450000	.925000
211	.012500	.250000	.400000	.700000
221	.012500	.250000	.525000	.775000
222	.012500	.250000	.450000	.925000
232	.012500	.250000	.550000	.950000
321	.006250	.175000	.525000	.775000
322	.006250	.175000	.450000	.925000
332	.006250	.175000	.550000	.950000

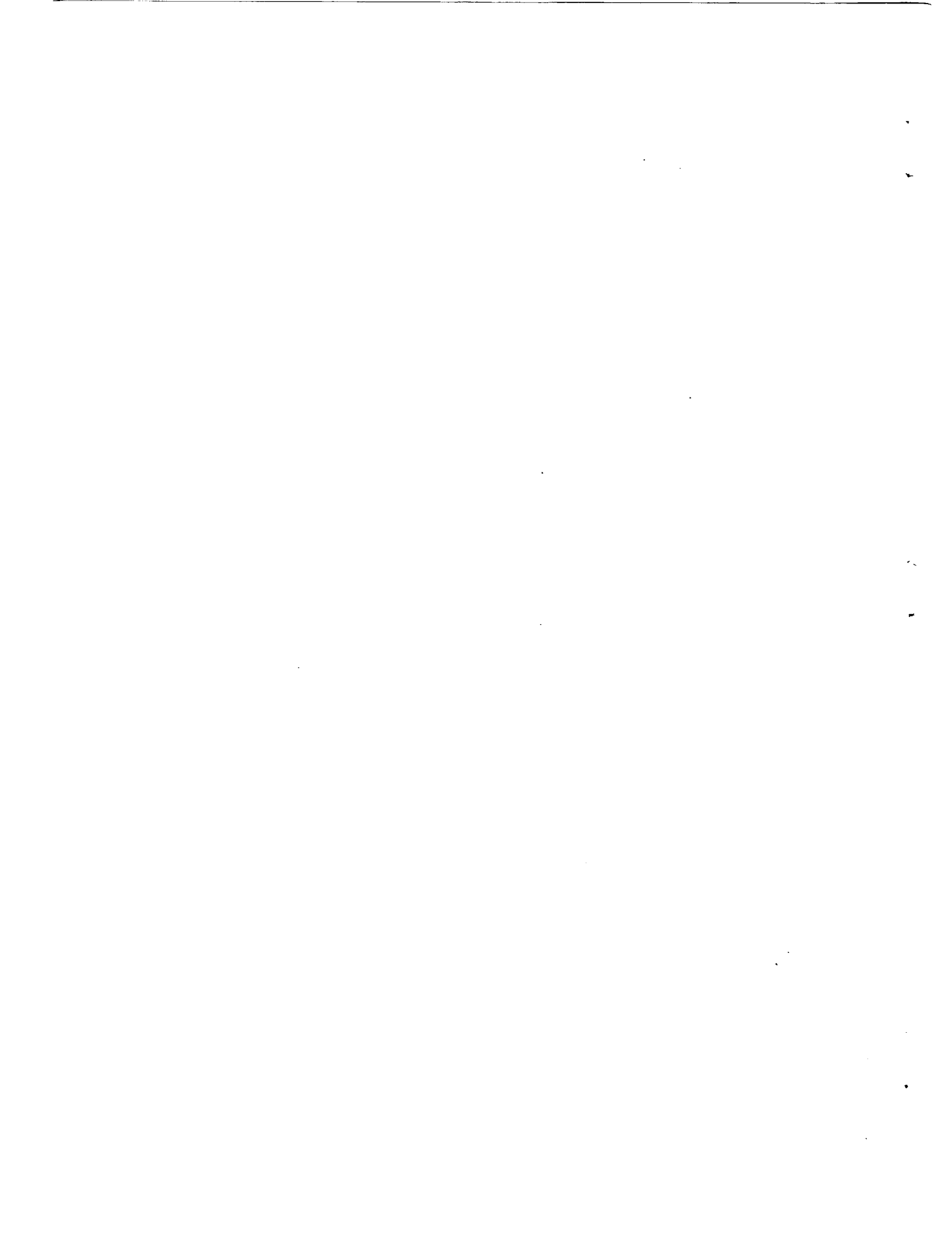


TABLE II

COMPUTED ORDINATES OF FUSELAGE FORMS  
[All values given as percentage of basic length. Basic length of models was 40 inches]

Form	111	a121	b122	s211	221	222	232	321	322	332
Station	Radius at specified stations									
-A	0	0	0	0	0	0	0	0	0	0
0	-	-	-	-	2.725	2.735	2.695	2.845	2.850	2.825
1.25	2.075	2.030	2.040	2.950	3.890	3.900	3.875	4.885	4.890	4.865
2.50	3.135	3.080	3.085	4.805	4.745	4.755	4.730	5.690	5.695	5.670
5.00	4.700	4.630	4.640	6.085	6.025	6.035	6.005	6.385	6.390	6.365
10.00	6.725	6.640	6.650	7.755	7.695	7.700	7.670	8.395	8.400	8.375
20.00	8.830	8.790	8.800	9.425	9.365	9.370	9.335	9.640	9.645	9.620
30.00	9.500	9.715	9.725	9.940	9.885	9.900	9.865	9.940	9.945	9.925
B	10.000	10.000	10.000	10.000	10.000	10.000	10.000	10.000	10.000	10.000
40	-	9.980	9.990	9.970	-	9.990	-	-	-	-
50	9.700	9.950	9.920	9.650	9.930	9.895	9.980	9.915	9.875	9.970
60	8.875	9.565	9.535	8.810	9.540	9.500	9.780	9.515	9.470	9.760
70	7.350	8.255	8.730	7.290	8.485	8.590	9.190	8.460	8.660	9.170
80	5.245	6.475	7.370	5.095	6.450	7.335	8.000	6.430	7.310	7.985
85	3.930	5.055	6.375	3.890	5.035	6.345	7.080	5.020	6.325	7.070
90	2.655	3.475	5.030	2.630	3.460	5.005	5.810	3.450	4.990	5.800
95	1.340	1.805	3.055	1.330	1.800	3.035	3.910	1.800	3.025	3.895
97.5	0.675	0.920	1.715	0	1.670	1.700	2.460	0	1.690	2.455
100	0	0	0	0	0	0	0	0	0	0
A	0.18	0.17	0.17	1.19	1.17	1.17	1.15	1.91	1.88	1.39
B	38.83	43.81	42.87	36.12	41.05	40.02	43.90	39.32	38.35	42.00

<sup>a</sup>The ordinates of models 121 and 211 as tested differ from the computed ordinates as tabulated because these models were obtained by combining nose and tail portions of other models; the separation between nose and tail portions was at station 3. The model tested as 121 was made up of the nose of model 111 and the tail of model 221, and the one tested as model 211 was made up of the nose of model 222 and the tail of model 111.

<sup>b</sup>Not tested.

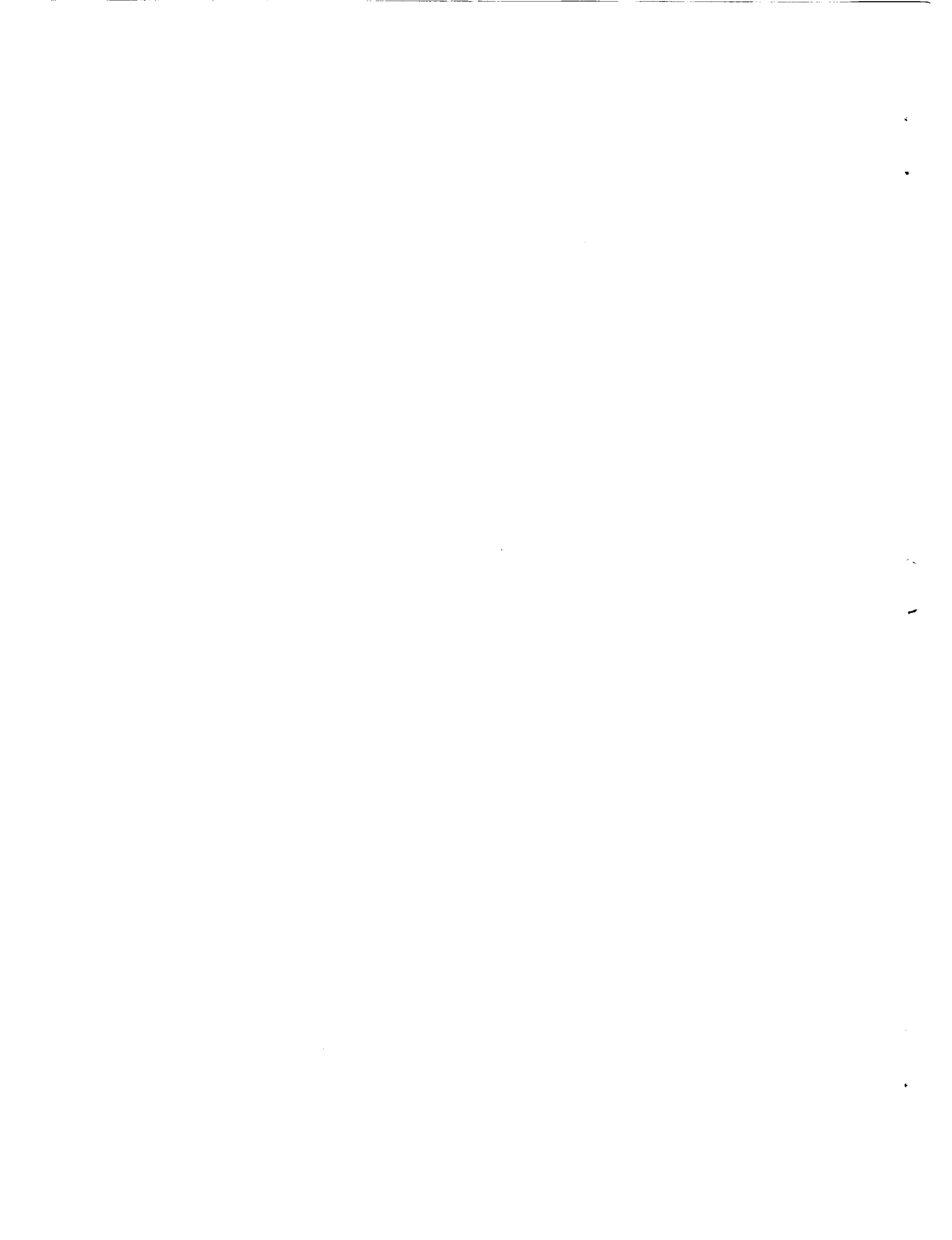
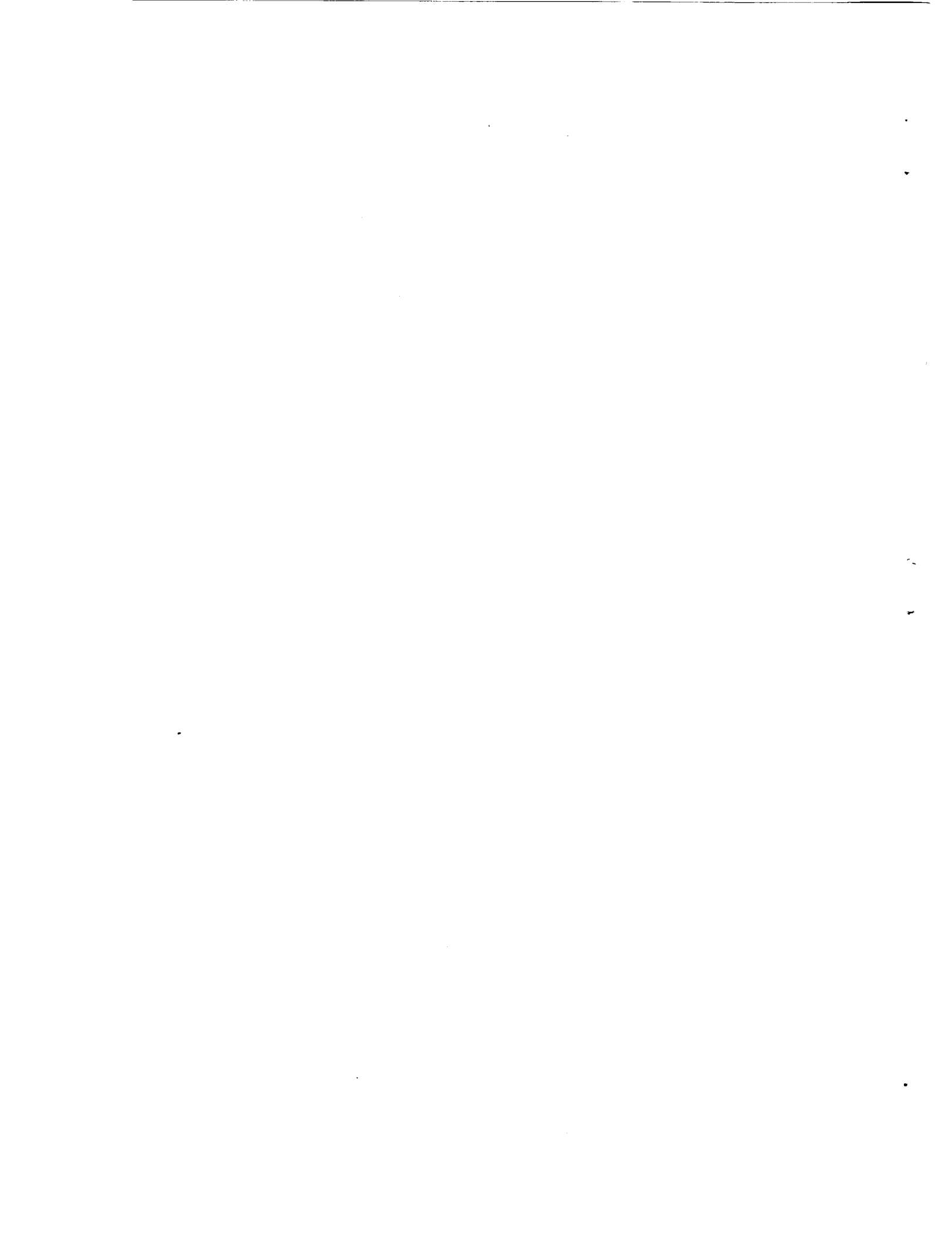


TABLE III  
 DRAG COEFFICIENTS AT AN EFFECTIVE  
 REYNOLDS NUMBER OF 66,000,000  
 (Reynolds Number is based on fuselage length)

Form	$C_D$	$C_{D_A}$
111	0.0179	0.0401
121	.0176	.0405
211	.0177	.0415
221	.0178	.0437
222	.0186	.0472
332	.0193	.0508



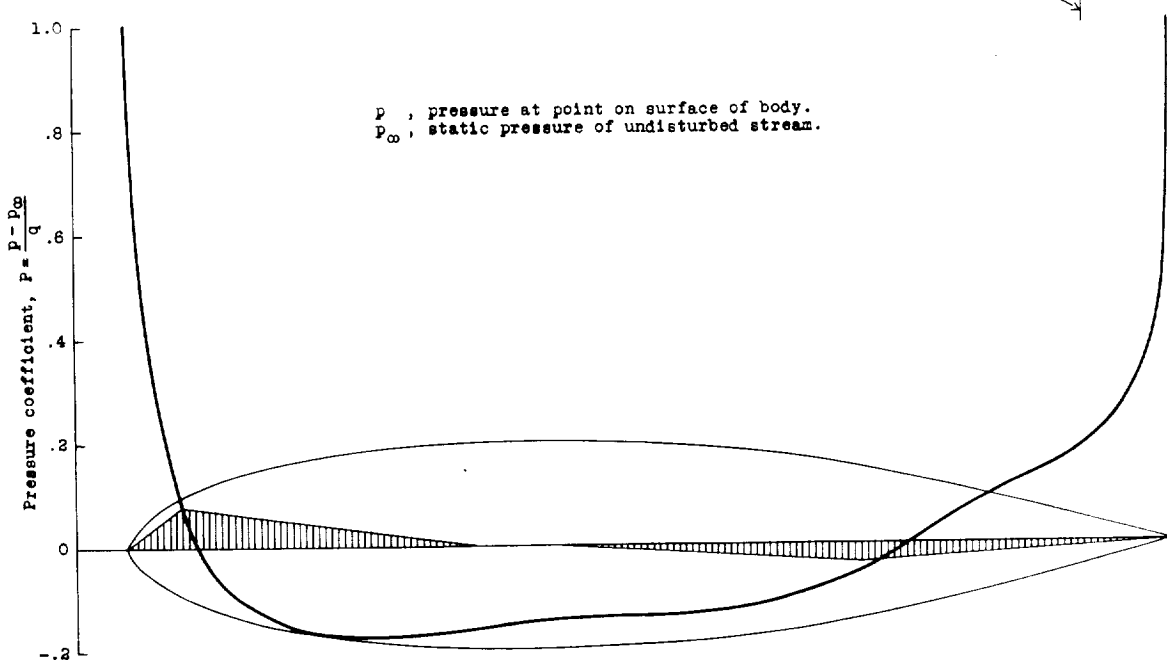
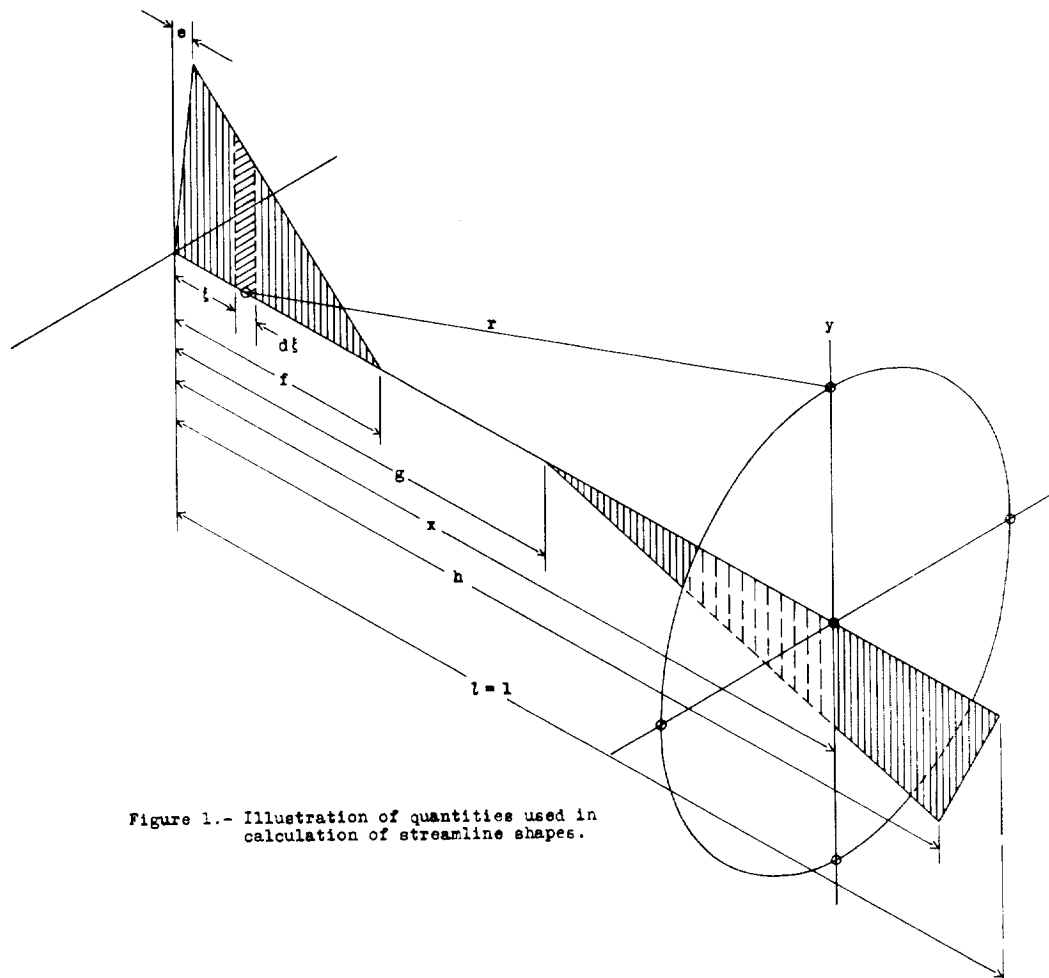
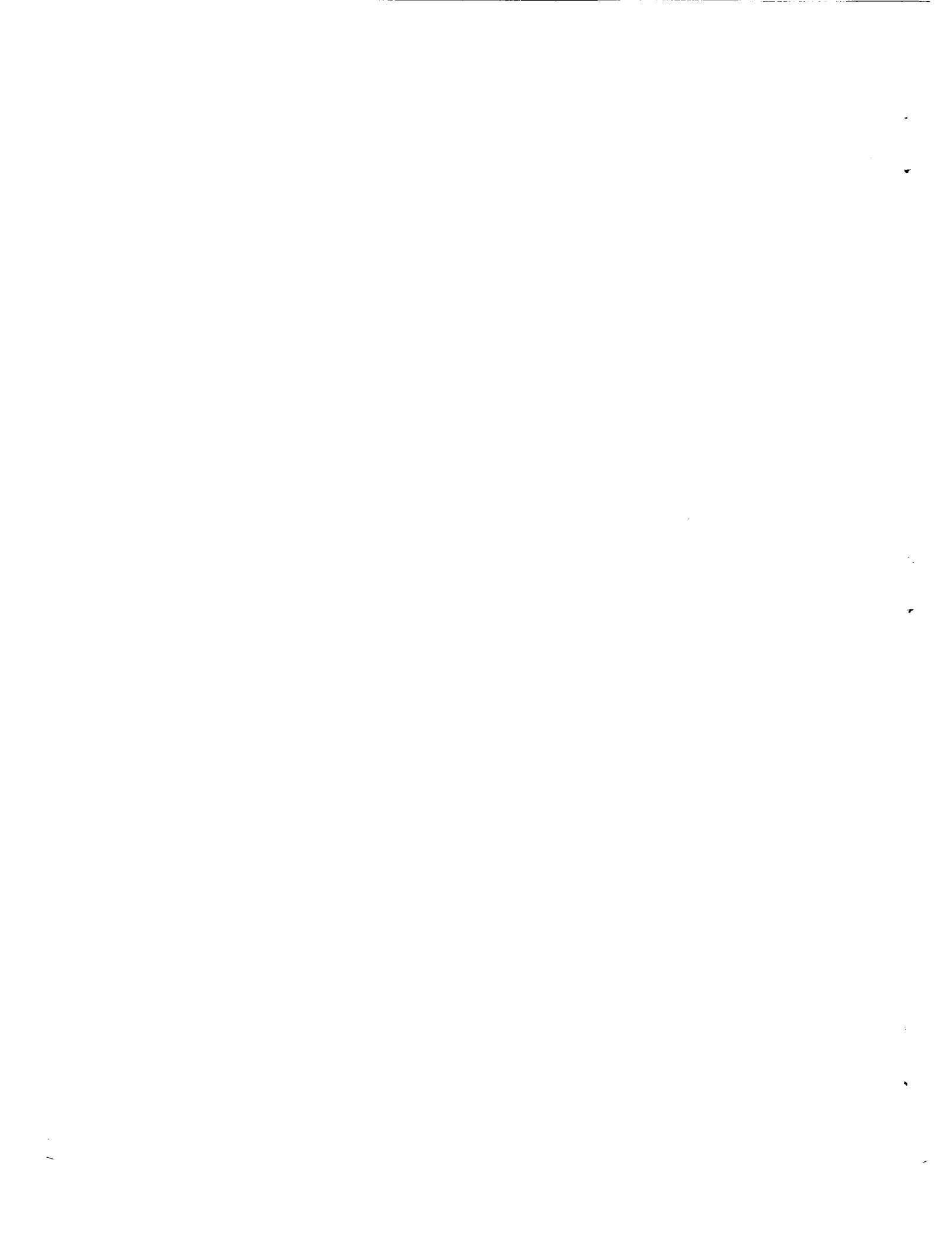


Figure 4.- Theoretical pressure distribution about form III.



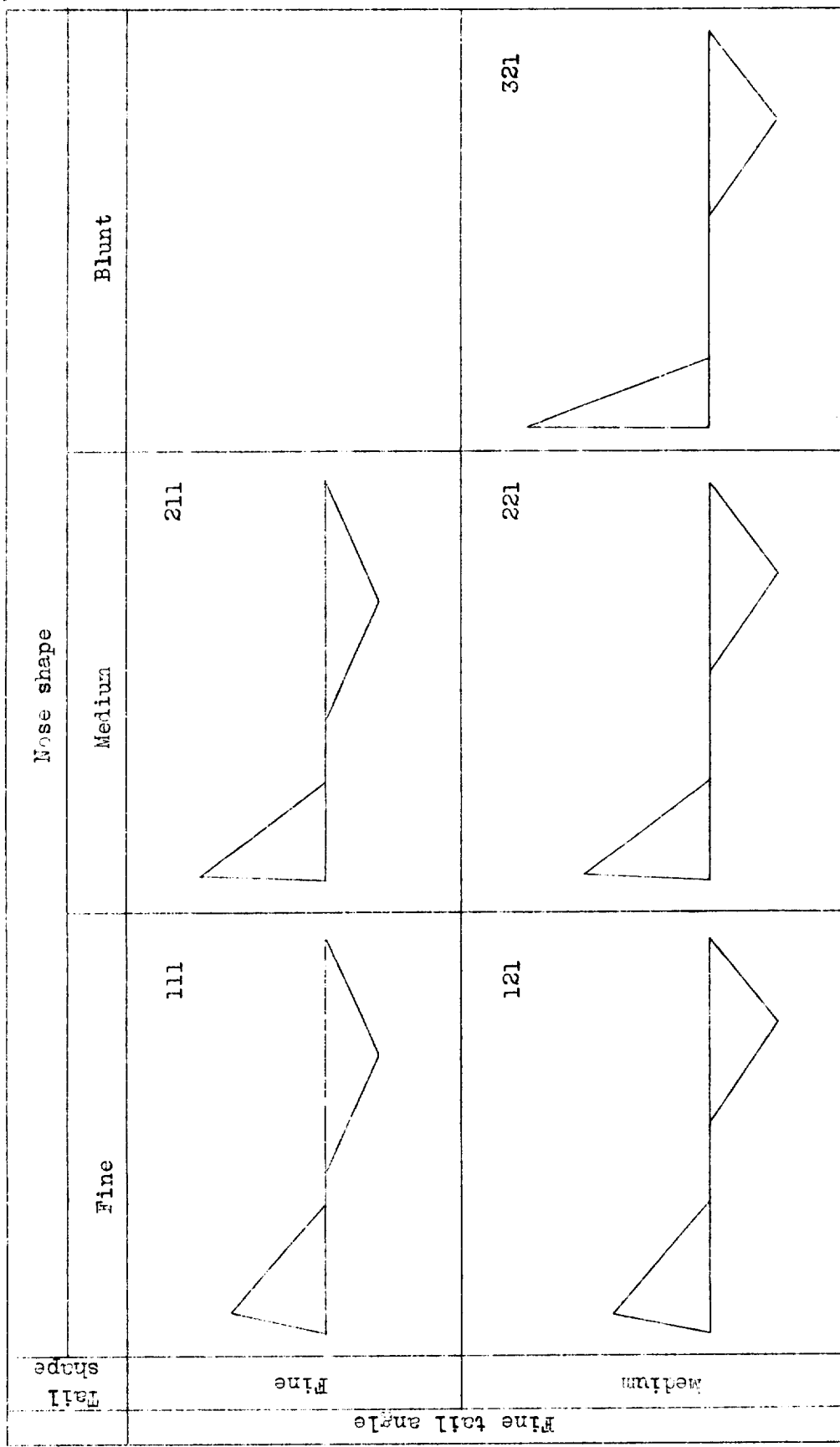
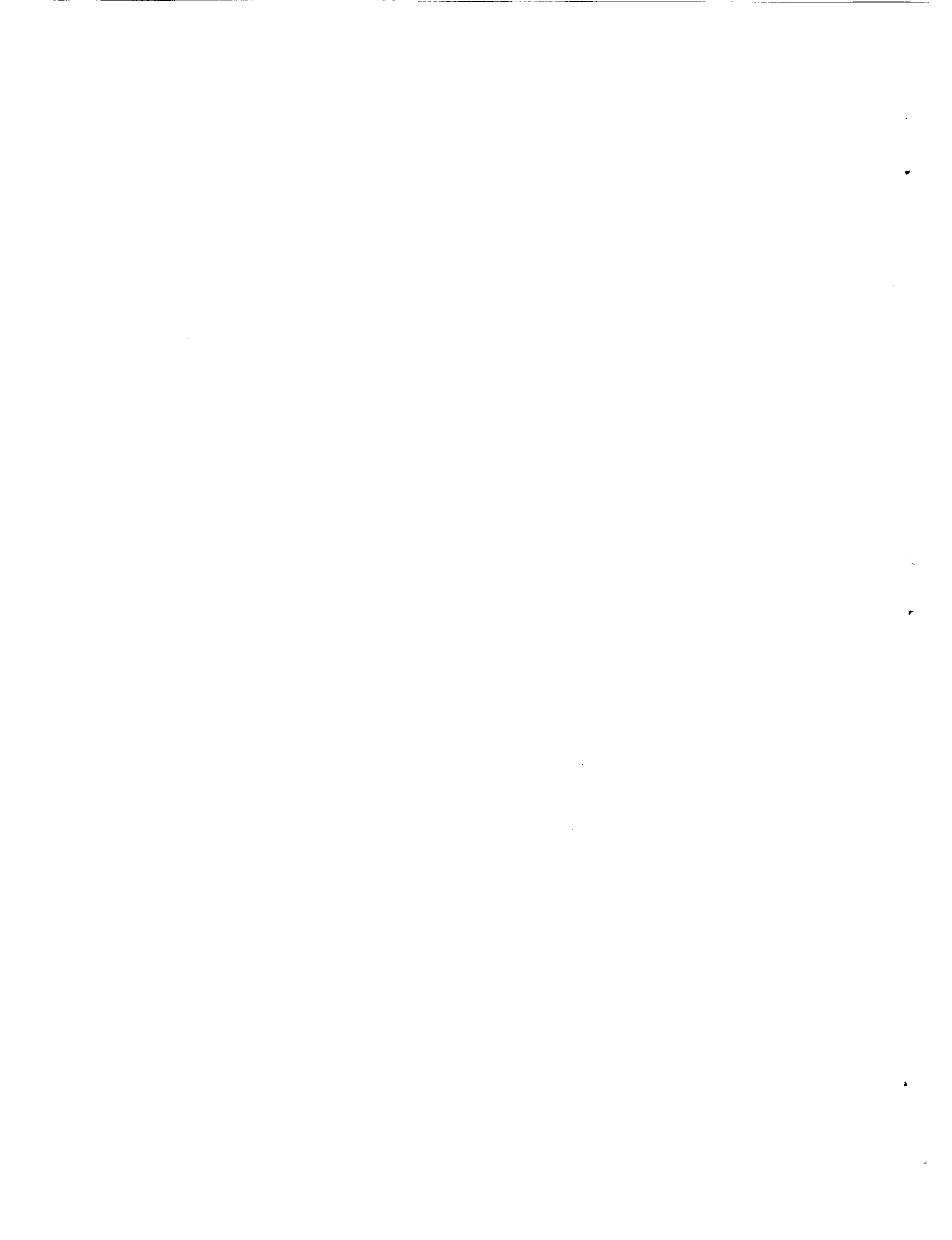


Figure 2a.— Source-sink distributions N.A.C.A. fuselage forms.



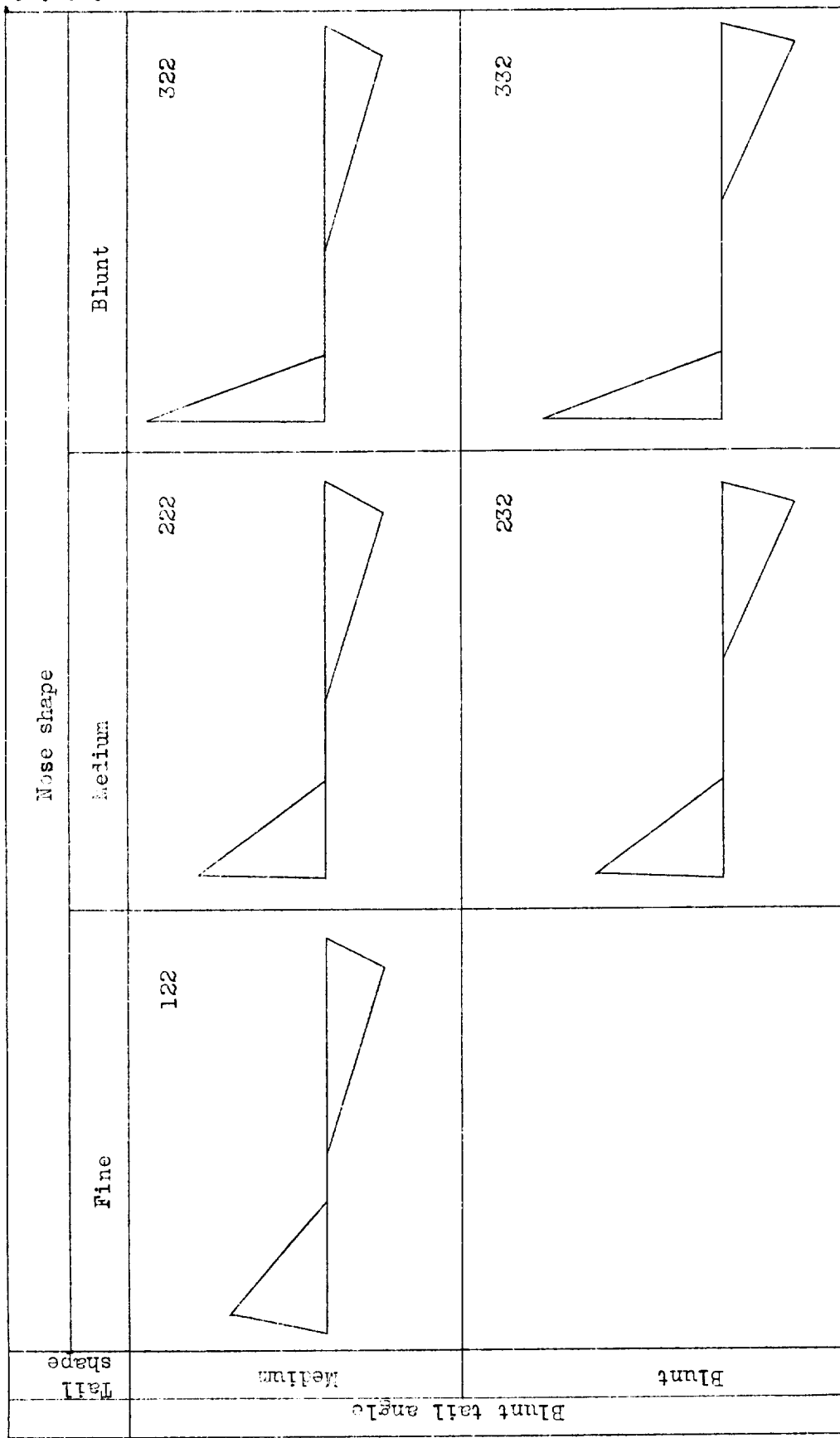
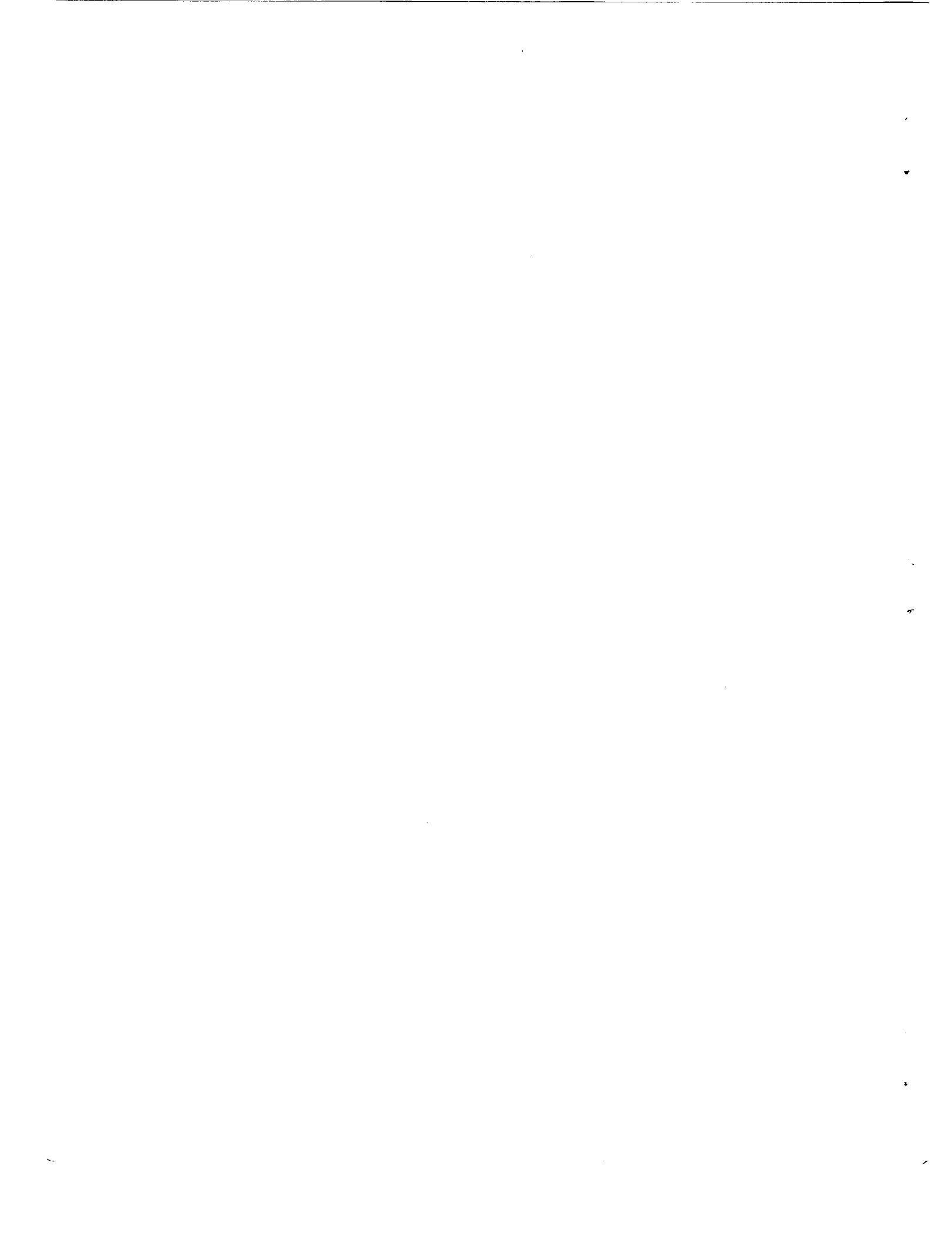


Figure 2b.— Source-sink distributions N.A.C.A. fuselage forms.



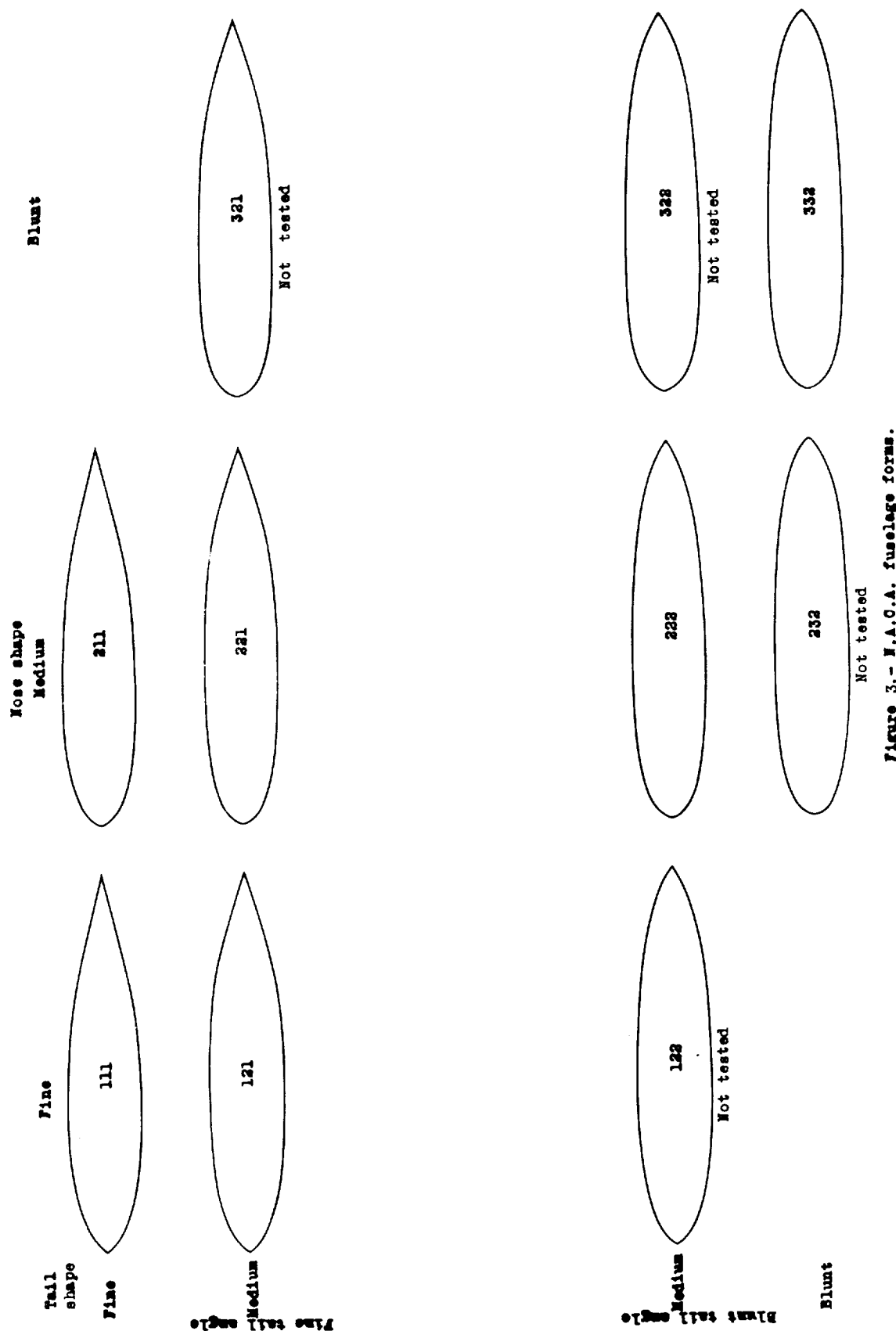
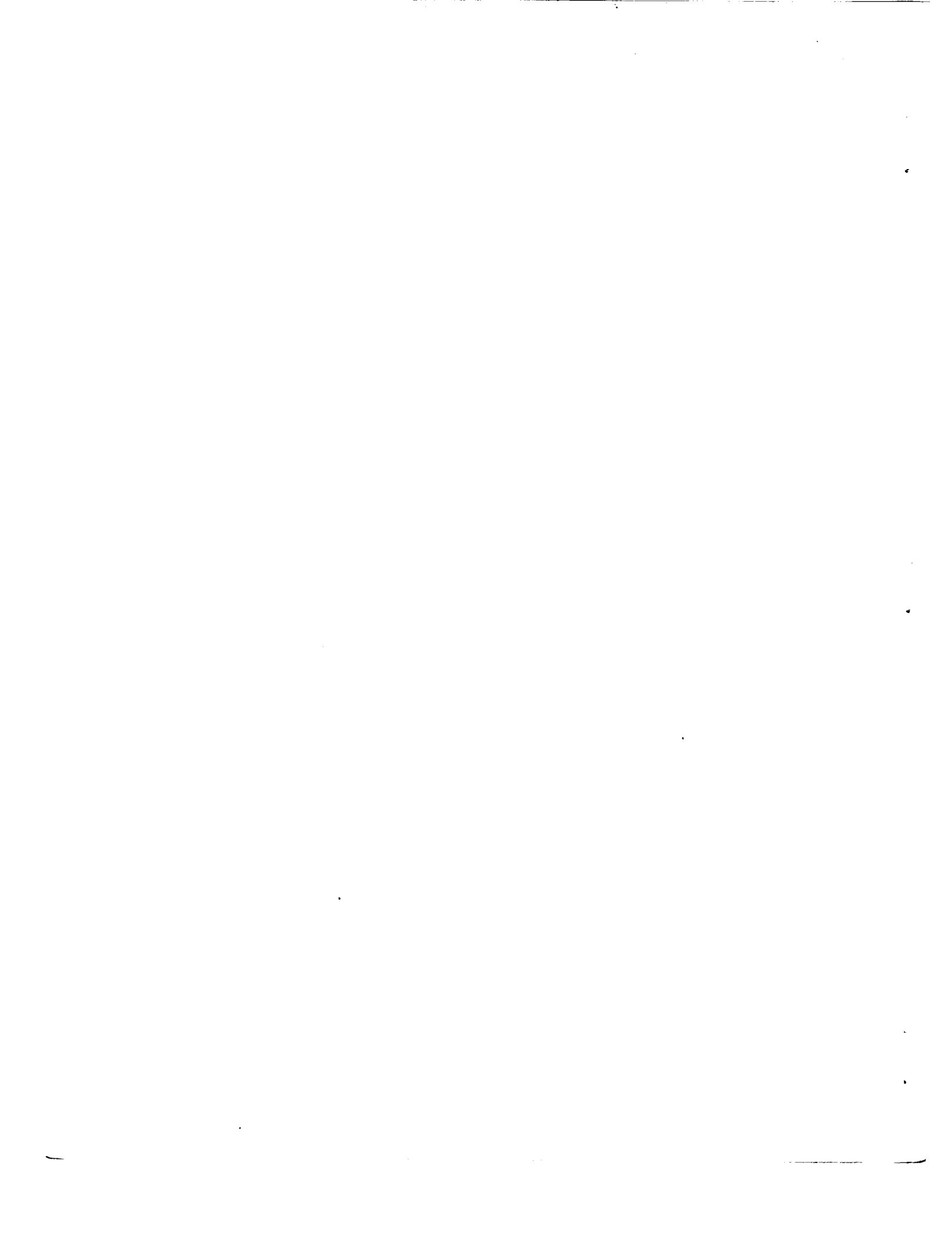


Figure 3.— N.A.C.A. fuselage forms.



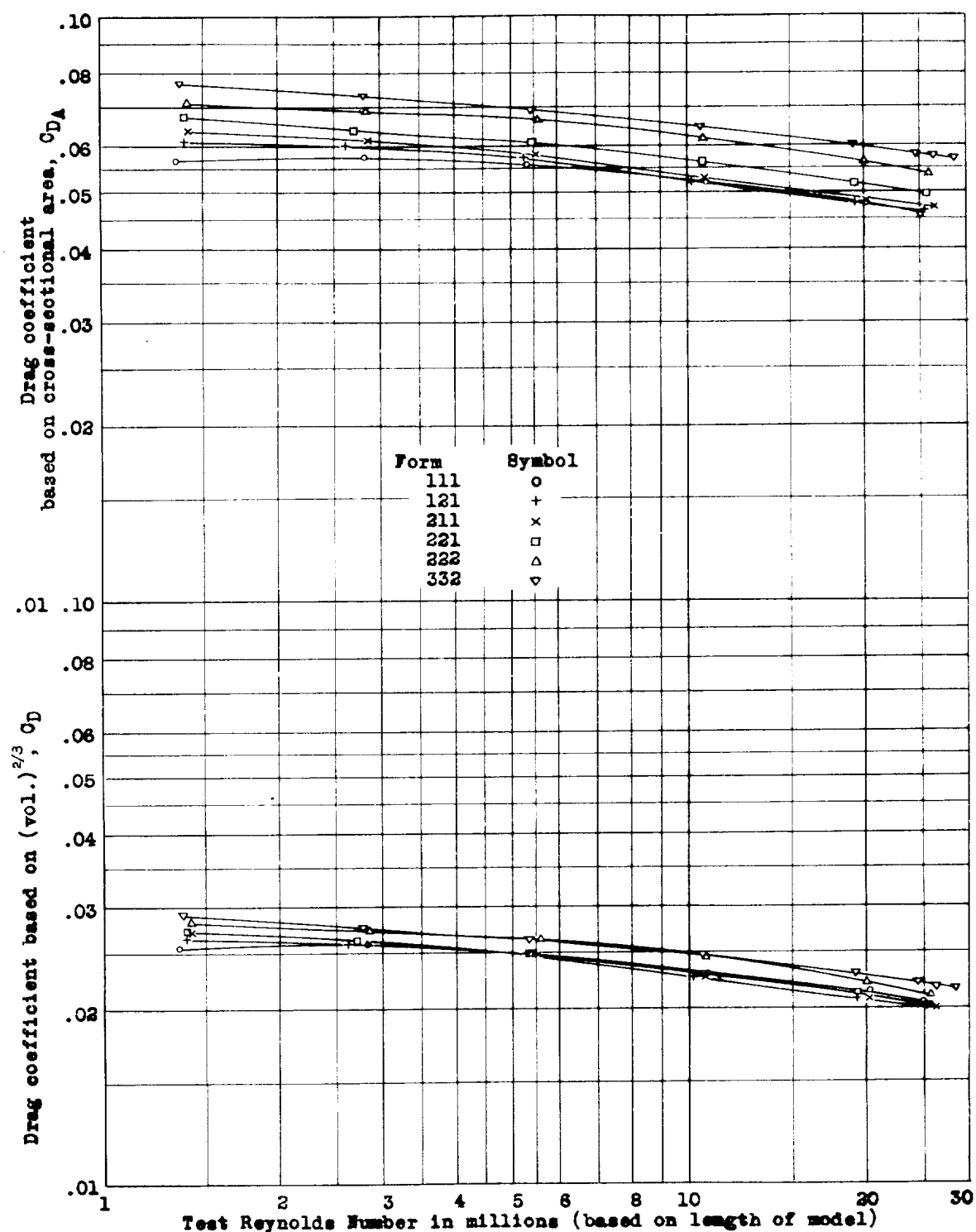


Figure 5.- Drag coefficients of N.A.C.A. fuselage forms.

